A Variational Approach to Spatially Dependent Non-Rigid Registration

Florian Jäger[a], Jingfeng Han[a], Joachim Hornegger[a] and Torsten Kuwert[b]

[a]Friedrich-Alexander-Universität Erlangen-Nürnberg, Institute of Pattern Recognition, Martensstraße 3, D-91058 Erlangen, Germany;
[b]Friedrich-Alexander-Universität Erlangen-Nürnberg, Nuclear Medicine, Krankenhausstraße 12, D-91054 Erlangen, Germany;

ABSTRACT

In this paper we propose a new variational non-rigid registration method that introduces prior knowledge about non-homogeneous deformation properties into the matching process. State-of-the-art medical image registration approaches usually assume that the whole image domain is associated with a homogeneous deformation property, thus bone structure and soft tissue have the same stiffness for instance. However, this assumption is not valid in the majority of cases. In many applications the deformation properties can be estimated manually by the physician or by segmentation, beforehand. The presented non-rigid registration method integrates knowledge about the tissue directly into the deformation field computation. For this reason, no additional post-processing steps, like filtering of the deformation field, are required. In order to integrate the tissue constraints the regularizer is replaced by a novel spatially dependent smoother. Dependent on the location within the image, the smoother is able to explicitly adjust the rigidity. Thus, different tissue classes can be treated in the registration process. In order to pass the stiffness coefficients to the algorithm an additional mask image is used. The registration results are illustrated on synthetic data first to give a good intuition about the effectiveness of the proposed method. Finally, we illustrate the improvement of the registration using real clinical data. It is shown that the mono-modal intra-patient registration of PET images yields more reasonable results using a spatially dependent regularizer constraining the deformations of regions with high activity than using a normal curvature regularizer. Furthermore, the method is evaluated on multi-modal PET/CT registration problems.

Keywords: Non-Rigid Registration, Spatially Dependent Regularizer, Variational Registration Approach

1. DESCRIPTION OF PURPOSE

An important application of medical imaging is the detection and quantification of lesions. For this purpose, functional as well as morphological imaging techniques are used. Both kinds of modalities have their pros and cons. Functional imaging has the advantage that regions with high activity, like malign lesions for instance, are easily detected in the data-sets. However, the spatial resolution and the tissue contrast of modalities like Positron Emission Tomography (PET) are very limited. For this reason, physicians are able to detect active regions in the images but they cannot localize and quantify them precisely. However, this is crucial for further treatments (e.g. ablation) and therapy control (follow-up studies). On the other hand, morphological imaging like Computerized Tomography (CT) has a high spatial resolution and tissue contrast. With that it is possible to do very precise measurements and to navigate easily within the volume. At the same time it is often hard to distinguish malign and benign tumors for instance as the absorbtion coefficient does not depend on the metabolic activity of the tissue.

Further author information:
F. Jäger: E-mail: jaeger@informatik.uni-erlangen.de, Telephone: +49 9131 85 27894
J. Han: E-mail: jingfeng@informatik.uni-erlangen.de, Telephone: +49 9131 85 27826
J. Hornegger: E-mail: hornegger@informatik.uni-erlangen.de, Telephone: +49 9131 85 27883
T. Kuwert: E-mail: torsten.kuwert@nuklear.imed.uni-erlangen.de, Telephone: +49 9131 85 33411

In order to solve this problem morphological and functional data-sets have to be aligned to each other and thus structural and metabolic information can be utilized in parallel. At present the registration of the data-sets is usually performed manually by the physician and the transformations used are kept rigid. As the acquisition times for a CT- (15-20 seconds) and a PET-Scan (15-30 minutes) differ very much, the volumes cannot be matched rigidly in general. CT-images are usually acquired with maximum inspiration whereas for PET the mean of the breathing cycles is used. Furthermore, the acquisition of the CT-volume is performed in an arms-up position and arms-down for PET. This yields non-linear deformations between the data-sets. Additionally, the manual alignment of the volumes leads to a considerable inter– and intra–observer variability.[1]

A solution to this problem is non-rigid multi-modal image registration. However, state–of–the–art algorithms imply a homogeneous stiffness in the whole image domain. This means that rigid structures, like bones, are warped in the same way as soft deformable structures, like muscles, skin, etc. For many applications this assumption does not yield reasonable deformation results. In PET imaging the shape of highly active regions differs very much for inter– as well as intra–patient measurements. Furthermore, active regions are not covering whole organs, like the heart for instance. For this reason, highly active regions have to be kept more rigidly during the registration process than areas with lower activity. Using current non-rigid methods, that do not utilize prior knowledge to register PET/CT images, lead to a false deformation of many areas of the moving image. The registration approach presented in this paper solves this problem by introducing a new regularizer that is spatially dependent. Thus, large stiffness coefficients can be assigned to regions with high activity.

2. METHODS

Image registration can be summarized as the problem of finding a deformation between a reference image R and a template image T so that the deformed template image T_φ is similar regarding a certain distance measure $\mathcal{D}$. The used distance measure depends on the application, the most common ones are the sum of squared differences (SSD), the normalized cross correlation (NCC) and mutual information (MI). SSD is mainly used for mono-modal registration purposes whereas NCC and MI are used for multi-modal matching applications. In this article we use SSD to demonstrate the applicability of the proposed registration method with artificial data-sets. Furthermore, the registration of the CT and PET volumes utilizes NCC and MI. However, the minimization of the proposed distance measures yields an ill-posed optimization problem. For this reason, further regularization terms have to be added to smooth the objective function. These so-called smoothers restrict the deformation of the template image in general. Mostly either elastic, fluid, curvature or diffusion approaches are utilized. State–of–the–art methods usually punish the deformation in every region in an equal manner. This, however, does not use prior information about certain tissue properties needed to find the correct minimum of the objective function. That leads either to a false deformation of rigid tissue if the influence of the regularizer is too small or an incorrect transformation of non-rigid tissue if it is too strict. In order to incorporate prior knowledge into the registration process some authors do adaptive filtering of the deformation field. Filtering of the deformation field is equivalent to the restriction using a curvature based smoother. Others include rigid regions into the non-rigid registration approach. With that it is possible to simulate bone structures like the spine for instance. Similar to the proposed method Bernd Fischer *et.al.* add a mask image containing the stiffness of the tissue into the registration process. They extended an elastic regularizer for this purpose. Christoph Gütter *et.al.* utilize prior knowledge for the registration of CT and PET images by adding a further smoother to the objective function.[2] This smoother corresponds to the Kullback Leibler (KL) distance of the joint histogram of both volumes to a previously learned reference joint histogram.

2.1. Segmentation

In this article we use a similar method to Bernd Fischer *et.al.*. The proposed algorithm can be separated into two distinct steps. First, a probability map is created that contains the information about the rigidity of the different tissue classes in the moving image. Usually the metabolic active regions contain the relevant medical information, thus these areas have to be kept more rigidly in the adaption process. With that the probability of being an active region correlates with the stiffness constraints. In order to gain the map, we are using a fuzzy-c-means approach.[3] There the volume is divided into N_c classes with the class centers c_i with $1 \leq i \leq N_c$. Furthermore each sample y_k (here voxel) has a membership probability $a_{i,k}$ to the class i. This means, that a single voxel belongs to every class with a certain probability. Thus the objective function J can be formulated as

$$J = \sum_{i=1}^{N_c} \sum_{k=1}^{n} a_{i,k}^{p} \|y_k - c_i\|^2 \tag{1}$$

subject to the probability constraints

$$\sum_{i} a_{i,k} = 1 \quad \text{and} \quad a_{i,k} \geq 0, \tag{2}$$

where p controls the fuzzyness of the result and $n = n_1 n_2 n_3$ is the number of the samples (here voxels), with (n_1, n_2, n_3) being the dimensionality of the regarded volumes. The goal is to find the class centers c_i and the partition matrix $a_{i,k}$ that minimize J. In the following the voxels are ordered in a lexicographic way in a vector $Y = (y_1, y_2, \ldots, y_n)^T$.[4] The proposed algorithm has the disadvantage that all voxels are treated in an independent manner and spatial coherency is not used for the classification. For this reason, we use a modified fuzzy-c-means approach introduced by Ahmed, Yamany, *et.al.* which includes the neighborhood of a voxel in the optimization process. The new objective function for clustering the PET image can be written as

$$J = \sum_{i=1}^{N_c} \sum_{k=1}^{n} a_{i,k}^{m} \|y_k - c_i\|^2 + \frac{\lambda}{N_R} \sum_{i=1}^{N_c} \sum_{k=1}^{n} a_{i,k}^{m} \sum_{y_r \in \mathcal{N}_{\mathcal{R}}} \|y_r - c_i\|^2 \rightarrow \min, \tag{3}$$

subject to the probability constraints

$$\sum_{i} a_{i,k} = 1 \quad \text{and} \quad a_{i,k} \geq 0, \tag{4}$$

with λ representing the influence of the neighborhood $\mathcal{N}_{\mathcal{R}}$ and N_R being the cardinality of $\mathcal{N}_{\mathcal{R}}$. The membership of the voxels to the class corresponding to the active regions is used as probability map. As metabolic highly active regions have large intensity values within the PET volume, the class κ can be computed with $\kappa = \arg\max_i c_i$.

2.2. Spatially dependent registration

In the second phase, the data–sets are registered using the mask image to constrain the deformation in certain regions of the PET volume. The method used is based on the variational registration approach introduced by J. Modersitzki.[4] Hence the optimization problem can be formulated as

$$\mathcal{J}[\vec{u}; T, R] = \mathcal{D}[\vec{u}; T, R] + \alpha \mathcal{S}[\vec{u}], \tag{5}$$

where the function $\vec{u} : \mathbb{R}^d \mapsto \mathbb{R}^d$ corresponds to the deformation field, d is the dimensionality of the data (we just use 3-d volumes, thus $d = 3$), T is the template image and R the reference image. Furthermore, $\mathcal{D}$ is the distance measure and $\mathcal{S}$ represents the smoother. The factor α defines the influence of the regularizer to the objective function. As both images can be seen as functions $f : \mathbb{R}^d \mapsto \mathbb{R}$, the deformed image T_φ can be computed as $T_\varphi(\vec{x}) = T \circ \varphi(\vec{x})$ with $\varphi(\vec{x}) = \vec{x} - \vec{u}(\vec{x})$.

In order to compute the similarity of the CT and the PET volumes, we use NCC and MI as distance measures. For the registration of artificial data-sets, we use SSD that is defined as

$$\mathcal{D}^{SSD}[\vec{u}; T, R] = \frac{1}{2} \int_\Omega (T_\varphi(\vec{x}) - R(\vec{x}))^2 d\vec{x}. \tag{6}$$

It calculates the distance between the volumes related to their intensity values, with Ω representing the image domain. Thus it is only suited for mono-modal cases. The similarity measure

$$\mathcal{D}^{NCC}[\vec{u}; T, R] = -\int_\Omega \frac{< R(\mathcal{X}(\vec{x})), T_\varphi(\mathcal{X}(\vec{x})) >}{\sqrt{< R(\mathcal{X}(\vec{x})), R(\mathcal{X}(\vec{x})) >< T_\varphi(\mathcal{X}(\vec{x})), T_\varphi(\mathcal{X}(\vec{x})) >}} d\vec{x} \tag{7}$$

computes the linear dependence of the data-sets,[5] with $\mathcal{X}$ being a local neighborhood around the vector $\vec{x}$. Therefor, it is applicable to mono-modal aswell as for multi-modal applications. The last distance measure

$$\mathcal{D}^{MI}[\vec{u};T,R] = \int_{\mathbb{R}^2} -p_{R,T_\varphi}(r,t)\log\frac{p_{R,T_\varphi}(r,t)}{p_R(r)p_{T_\varphi}(t)}drdt, \tag{8}$$

maximizes the statistical dependence between the CT and PET volume.[6] Here $p_{R,T_\varphi}(r,t)$ is the joint histogram of the reference and the deformed template image $p_R(r) = \int_{\mathbb{R}} p_{R,T_\varphi}(r,t)dt$ and $p_{T_\varphi}(t) = \int_{\mathbb{R}} p_{R,T_\varphi}(r,t)dr$ are its marginalizations.

In order to find the minimum of the objective function $\mathcal{J}$, a variational problem of first order has to be solved. Therefor, the Gâteaux derivative has to be applied to $\mathcal{J}$. Thus the proposed distance measures yield (see Modersitzki *et.al.*,[?] Hermosillo *et.al.*[7])

$$\begin{aligned}
f^{SSD}(\vec{x},\vec{u}(\vec{x})) &= d\mathcal{D}^{SSD}[\vec{u};T,R] = (R(\vec{x}) - T_\varphi(\vec{x}))\nabla T_\varphi(\vec{x}), & (9)\\
f^{NCC}(\vec{x},\vec{u}(\vec{x})) &= d\mathcal{D}^{NCC}[\vec{u};T,R] = \frac{\sum_{i\in\mathcal{X}(\vec{x})}(T_\varphi(\vec{x_i}) - R(\vec{x_i})\gamma_1)\nabla T_\varphi(\vec{x_i})}{\sqrt{< R(\mathcal{X}(\vec{x})), R(\mathcal{X}(\vec{x})) >< T_\varphi(\mathcal{X}(\vec{x})), T_\varphi(\mathcal{X}(\vec{x})) >}} & (10)\\
\text{with} \quad \gamma_1 &= < R(\mathcal{X}(\vec{x})), T_\varphi(\mathcal{X}(\vec{x})) >,\\
f^{MI}(\vec{x},\vec{u}(\vec{x})) &= d\mathcal{D}^{MI}[\vec{u};T,R] = \frac{1}{\|\Omega\|}\left(\frac{\partial_2 p_{R,T_\varphi}(r,t)}{p_{R,T_\varphi}(r,t)} - \frac{p'_{T_\varphi}(t)}{p_{T_\varphi}(t)}\right)\nabla T_\varphi(\vec{x}), & (11)
\end{aligned}$$

where the operator $d\mathcal{D}$ is the Gâteaux derivative and $\partial_2 p_{R,T_\varphi}(r,t)$ denotes the partial derivative of $p_{R,T_\varphi}(r,t)$ with respect to its second variable.

In order to constrain the deformation according to the stiffness coefficients the standard regularizers were replaced by a novel spatially dependent smoother. However, the used regularizer bases on the curvature smoother. The spatial dependency is realized by integrating a continuously differentiable function $b : \mathbb{R}^d \mapsto \mathbb{R}$ that depends on the position in the template image. This function includes the prior information about the membership of a voxel to an active region gained by the fuzzy-c-means segmentation step beforehand. The spatial dependent regularizer can be formulated as

$$\mathcal{S}^{spatial}[\vec{u}] := \frac{1}{2}\sum_{l=1}^{d}\int_\Omega b(\varphi(\vec{x}))(\triangle u_l)^2 d\vec{x}. \tag{12}$$

where the operator $\triangle$ represents the Laplace operator $\triangle f = \sum_{i=1}^{d}\partial_{x_i,x_i}f$. With that, the curvature of the deformation field is regularized stronger in regions with high function values of b, thus in areas with high metabolic activity within the PET volume. Nevertheless, affine linear transformations of these regions are still possible.

In order to solve the variational problem the Gâteaux derivative $d\mathcal{S}^{spatial}$ has to be computed. This results in

$$\mathcal{A}^{spatial}[\vec{u}] = d\mathcal{S}^{spatial}[\vec{u}] = b(\varphi(\vec{x}))\triangle^2\vec{u}. \tag{13}$$

Using one of the similarity measures (eqn 9, 10 and 11) and the proposed smoother (eqn 13) the solution to the variational optimization problem can be found by solving the Euler Lagrange equation

$$\mathcal{A}^{spatial}[\vec{u}] - f(\vec{x},\vec{u}(\vec{x})) = 0, \quad \text{for all} \quad \vec{x}\in\Omega, \tag{14}$$

Initialization: $R \leftarrow$ CT, $T \leftarrow <$ PET, $U \leftarrow 0$
Segmetation: Compute c_i and $a_{i,k}$ using eqn. 3
Compute probability map $a_{\kappa,i}$
Registration: $i < I_{max}$
Compute γ using eqn. 16
Update U using eqn. 15
$i \leftarrow i + 1$
return T_φ

Figure 1. Spatially dependent non-rigid registration

2.3. Implementation

The discrete version of the spatially dependent function b is defined as $b_{dis}(\vec{x}) = \alpha + \gamma a_{\kappa,j}$, with α being the initial stiffness of the tissue, γ controlling the influence of the spatial coherency and $a_{\kappa,j}$ being the probability of the membership of the voxel y_i to an active region of the PET image. With that the differential operator $\mathcal{A}^{spatial}$ (eqn. 13) can be discretized as the matrix product $A^{spatial} = BA^{curv}$, where B is a diagonal matrix that inherits the values of b_{dis} in lexicographic order and A^{curv} equals the discrete version of the curvature differential operator (see Modersitzki[?]). In the discrete version of the optimization problem, the deformation field is stored in $U = (\vec{u_1}, \vec{u_2}, \ldots, \vec{u_n})$, where $\vec{u_i}$ represents the i-th position in the deformation field in lexicographic ordering. Hence, the optimization problem of equation 14 can be formulated as

$$BA^{curv}U = F, \tag{15}$$

with F being the force vector $F = (\vec{f_1}, \vec{f_2}, \ldots, \vec{f_n})$, $f_i = f(y_i, u_i)$. However, due to the spatial dependency the solution to the partial differential equation optimization problem cannot be found using the discrete cosine transformation, like for the curvature registration for instance, but an explicit solution scheme has to be used.

One problem of the integration of spatial coherencies is that strongly constrained areas yield a very bad convergence property. For this reasen, we splitted the registration process in three different phases. First a unconstraint registration is performed, after half of the iterations the spatial dependency is increased linearly to its maximal extend. The actual factor γ can be computed by

$$\gamma = \gamma_{max} \frac{4(i - I_{max}/2)}{I_{max}}, \tag{16}$$

with γ_{max} being the maximal influence, i representing the actual iteration and I_{max} describing the maximal nuber of iterations. Finally, the spatial dependent registration is performed. Furthermore, it is difficult to find an appropriate stop criteria, as for the spatial regularization, there is always a difference between the images - otherwise standard smoothers can be used. Therefor, we performed a fixed number of iterations. The overall spatially dependent non-rigid registration algorithm is summarized in figure 1.

3. RESULTS

We evaluated our approach with three different registration problems. First, we showed that the spatial dependent registration algorithm is applicable on synthetic data-sets using SSD as similarity measure. Therefor, we created a reference data-sets inheriting two cubes and a template data-set with two spheres. The centers of the cubes and spheres differ. With that the registration approach has to translate the centers and deform the spheres to the cubes. In the first experiment we used a standard curvature based regularizer. That yielded a correct translation and deformation of both spheres as expected. In the next step we regularized one of the spheres to be nearly rigid. That yielded one correctly registered sphere (unconstrained). The constrained sphere was translated and

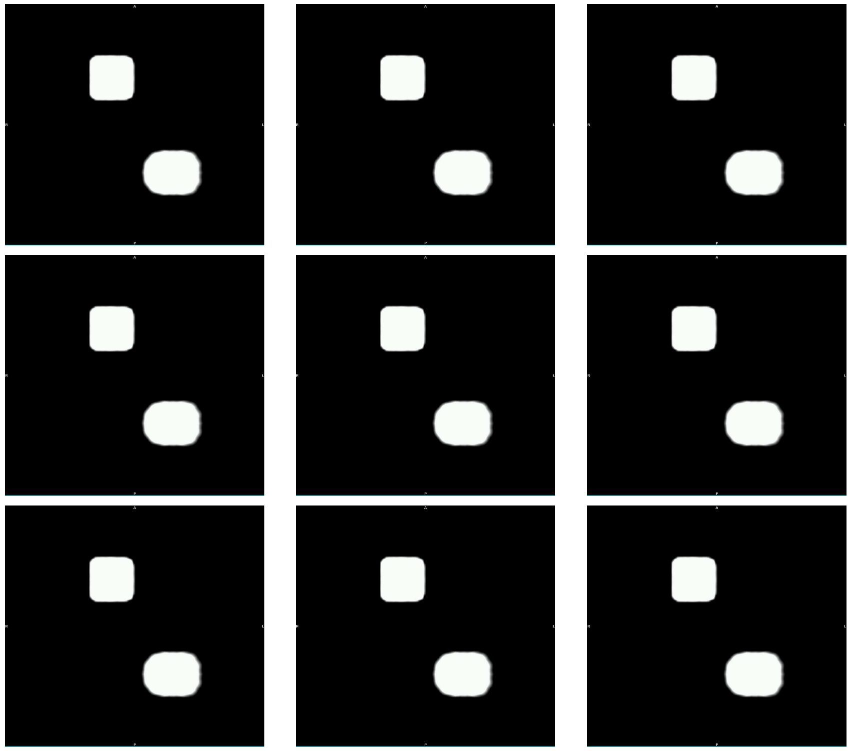

Figure 2. Registration result of artificial data-sets using SSD. Top row, from left to right: reference image, template image, mask image. Middle Row: the registration results before applying the spatial dependend smoother ($i = I_{max}/2$). From left to right: deformed template image without spatial constraints, T_φ with spatial constraints, deformed mask image. Bottom Row: result of he registration $i = I_{max}$ (images are the same as in the middle row).

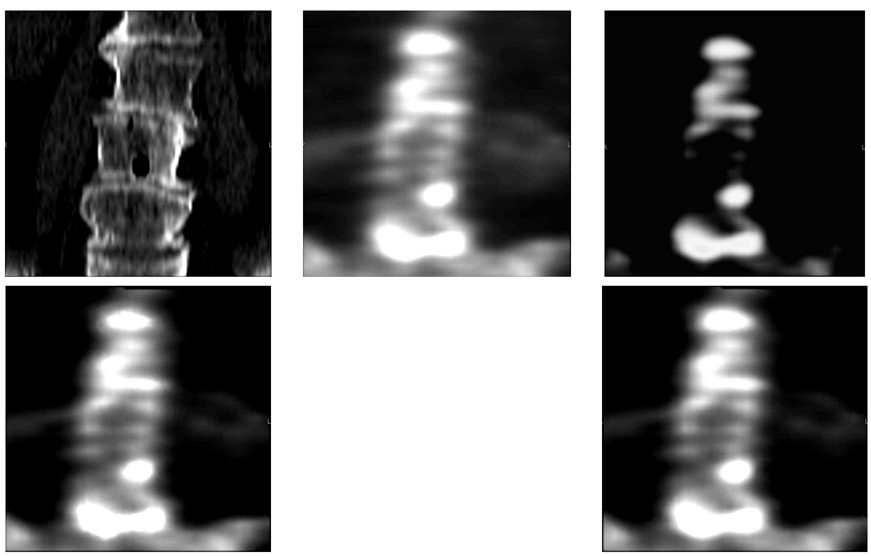

Figure 3. Korrespondierende Schichten eines zur Evaluierung verwendeten Datensatzes und das Ergebnis der Registrierung: Original CT Volumen (oben links), original SPECT Volumen (oben mitte), verwendete Wahrscheinlichkeitskarte (oben rechts), deformiertes Volumen ohne ortsabhngige Regularisierung (unten links) und mit ortsabhngiger Regularisierung (unten rechts).

.

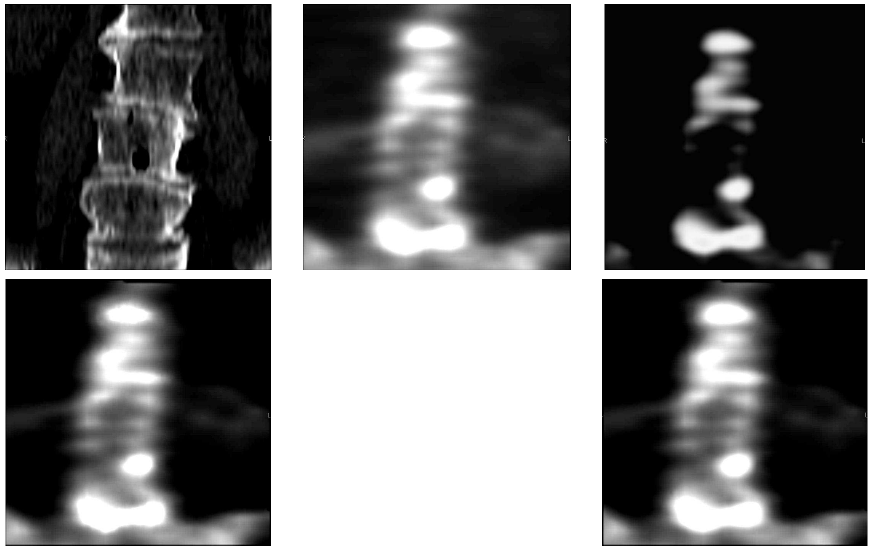

Figure 4. Korrespondierende Schichten eines zur Evaluierung verwendeten Datensatzes und das Ergebnis der Registrierung: Original CT Volumen (oben links), original SPECT Volumen (oben mitte), verwendete Wahrscheinlichkeitskarte (oben rechts), deformiertes Volumen ohne ortsabhngige Regularisierung (unten links) und mit ortsabhngiger Regularisierung (unten rechts).

.

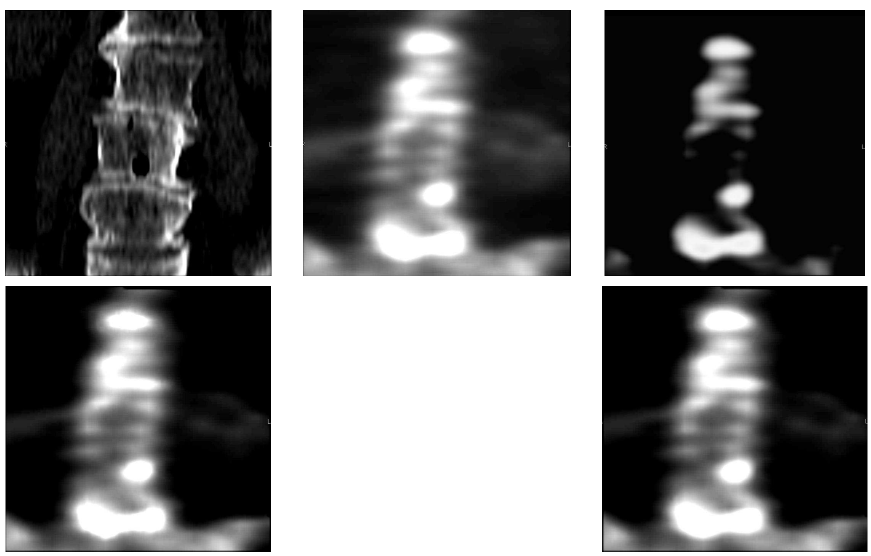

Figure 5. Korrespondierende Schichten eines zur Evaluierung verwendeten Datensatzes und das Ergebnis der Registrierung: Original CT Volumen (oben links), original SPECT Volumen (oben mitte), verwendete Wahrscheinlichkeitskarte (oben rechts), deformiertes Volumen ohne ortsabhngige Regularisierung (unten links) und mit ortsabhngiger Regularisierung (unten rechts).

.

scaled, but was not deformed too much anymore. Slight deformations were expected, as the second sphere was just regularized more strictly. The results of the registration using artificial data-sets are illustrated in figure 2. Then we did a mono-modal non-rigid PET/PET registration, labeling the regions with high activity as almost rigid. This yielded a smooth deformation field with little deformations in the labeled areas only. Finally, we used the approach to register PET/CT images with the focus to keep the deformations of high active regions reasonable. For instance, one serious problem is the alignment of the heart between the CT and the PET scan. Without a spatial dependency of the deformation field, it tends to a non-reasonable deformation in that area of the PET image. The results of the PET/CT registration are illustrated in figure 1. Here, the deformations of the heart were constrained. As expected the high active region and the heart itself did just slightly deform compared to the unconstrained case.

4. NEW OR BREAKTHROUGH WORK TO BE PRESENTED

The adapted regularizer for variational non-rigid registration enables differentiation of rigidity of different tissue classes by integrating prior knowledge into the alignment process. Thereby, it is not required to perform additional post-processing of the gained deformation field after each iteration. This means, that in comparison to other approaches that use prior knowledge for registration, the properties of all tissue classes are treated democratic and not iteratively. The knowledge is gained by a previous segmentation step (manually or automatically) and is then passed to the registration algorithm as a mask image that inherits the different stiffness coefficients.

5. CONCLUSIONS

We showed in this article that it is possible to integrate prior knowledge into the registration. With that, problems that occur during the alignment of PET/CT data-sets, like false deformations of the heart, can be solved. As the formulation of our approach is not designed for a specific problem, it can be used for many registration tasks where a classification of the stiffness coefficients of the tissue can be performed.[8941011 1271314]

6. ACKNOWLEDGMENT

We would like to thank Hipgraphics for their support and for providing the volume renderer InSpace at no charge. Furthermore, we would like to thank the Deutsche Forschungsgemeinschaft (DFG), SFB 603, subproject C10, for their financial support.

REFERENCES

1. A. Noemayr, W. Roemer, T. Hothorn, A. Pfahlberg, J. Hornegger, W. Bautz, and T. Kuwert, "Anatomical accuracy of lesion localization by retrospective interactive rigid image registration between F-18-FDG-PET and X-Ray CT," *Nuklearmedizin* **44**(4), pp. 149–155, 2005.
2. C. Gütter, C. Xu, F. Sauer, and J. Hornegger, "Non-rigid multi-modal image registration using kullback-leibler divergence," in *MICCAI*, (2), pp. 255–262, Springer-Verlag, (London, UK), 2005.
3. R. O. Duda, P. E. Hart, and D. G. Stork, *Pattern Classification*, Wiley, New York, 2000. 2nd Edition.
4. J. Modersitzki, *Numerical Methods for Image Registration*, Oxford University Press, Oxford New York, 2004.
5. J. Rexilius, S. K. Warfield, C. R. G. Guttmann, X. Wei, R. Benson, L. Wolfson, M. E. Shenton, H. Handels, and R. Kikinis, "A novel nonrigid registration algorithm and applications," in *MICCAI '01: Proceedings of the 4th International Conference on Medical Image Computing and Computer-Assisted Intervention*, pp. 923–931, Springer-Verlag, (London, UK), 2001.
6. W. Wells, P. Viola, H. Atsumi, S. Nakajima, and R. Kikinis, "Multi-modal volume registration by maximization of mutual information," *Medical Image Analysis* **1**(1), pp. 35–51, 1996.
7. G. Hermosillo, C. Chefd'hotel, and O. Faugeras, "Variational methods for multimodal image matching," *Int. J. Comput. Vision* **50**(3), pp. 329–343, 2002.
8. M. N. Ahmed, S. M. Yamany, N. Mohamed, A. A. Farag, and T. Moriarty, "A modified fuzzy c-means algorithm for bias field estimation and segmentation of MRI data," *IEEE Trans Med Imaging* **21**(3), pp. 193–199, 2002.

9. M. Staring, S. Klein, and J. P. Pluim, "Nonrigid registration with adaptive, content-based filtering of the deformation field," in *Proc of SPIE Medical Imaging*, **5747**, pp. 212–221, 2005.
10. S. Kabus, A. Franz, and B. Fischer, "On elastic image registration with varying material parameters," in *Procs BVM*, pp. 330–334, 2005.
11. J. A. Little, D. L. G. Hill, and D. J. Hawkes, "Deformations incorporating rigid structures," *j-COMP-VIS-IMAGE-UNDERSTANDING* **66**(2), pp. 223–232, 1997.
12. J. Maintz and M. Viergever, "A survey of medical image registration," *Medical Image Analysis* **2**(1), pp. 1–36, 1998.
13. U. Clarenz, M. Droske, S. Henn, M. Rumpf, and K. Witsch, "Computational methods for nonlinear image registration," *Mathematical methods in image registration, Mathematics in Industry, Springer* , 2005.
14. E. Suárez, C.-F. Westin, E. Rovaris, and J. Ruiz-Alzola, "Nonrigid registration using regularized matching weighted by local structure," in *MICCAI '02: Proceedings of the 5th International Conference on Medical Image Computing and Computer-Assisted Intervention-Part II*, pp. 581–589, Springer-Verlag, (London, UK), 2002.